

25th February 2025

Note added after first publication: This Supplementary Information file replaces that originally published 31st March 2021

Supporting Information

An unexpected role of an extra phenolic hydroxyl on the chemical reactivity and bioactivity of catechol or gallol modified hyaluronic acid hydrogels

Sumanta Samanta^[a], Vignesh K. Rangasami^[a], N. Arul Murugan^[b], Oommen P. Varghese^[c], and Oommen P. Oommen*^[a]

^[a] Bioengineering and Nanomedicine Lab, Faculty of Medicine and Health Technology, Tampere University, 33720 Tampere, Finland

^[b] Department of Theoretical Chemistry and Biology, School of Engineering Sciences in Chemistry, Biotechnology and Health, KTH Royal Institute of Technology, S-106 91 Stockholm, Sweden

^[c] Polymer Chemistry Division, Translational Chemical Biology Laboratory, Department of Chemistry, Ångström Laboratory, Uppsala University, 75121 Uppsala, Sweden

1. MATERIALS AND METHODS

Hyaluronic acid (MW 130 kDa) was purchased from LifeCore Biomedical (Chaska, USA). Gallic acid (3,4,5-trihydroxy benzoic acid), dopamine (2-(3,4-Dihydroxyphenyl) ethylamine hydrochloride), 1-ethyl-3-(3-dimethylamino propyl)-carbodiimide hydrochloride (EDC), 1-hydroxy benzotriazole hydrate (HOBt), N-hydroxysuccinimide (NHS), Carbohydrazide (CDH), Sodium periodate was purchased from Sigma-Aldrich. Dialysis membranes used for purification were purchased from Spectra Por-6 (MWCO 3500). All solvents were of analytical quality. All spectrophotometric analysis was carried out on Shimadzu UV-3600 plus UV-VIS-NIR spectrophotometer. All the solvents were of analytical quality. The NMR experiments (δ scale) were recorded with JEOL ECZR 500 instruments, operating at 500 MHz for ¹H. Spectra for GA-Hyd was recorded in DMSO-d₆ and all HA conjugates were recorded in D₂O at 293 K.

1.1 Computational Analysis

We have computed the energetics associated with deprotonation and free radical formation of dopamine and gallic acid derivatives (refer to structure 1 and 7 in Figure 1) by employing density functional theory with B3LYP and 6-311+G** level of theory.¹ To describe the solvent environment (aqueous solvent), we adopted the CPCM model.¹ The molecular structures for neutral, anion, and dianion forms and free radical and diradical forms were built using molden software.² The structures for water, hydronium ion, hydrogen peroxide, and peroxide-free radical were built in the same way. We performed the optimization of the geometries of all the neutral and charged and free radical forms. The structures optimized were confirmed to correspond to the energy minimum by computing the

normal modes. All the electronic structure calculations were performed by employing Gaussian09 software.³ The energies for all the molecular structures were computed with and without zero-point energy corrections and were used to compute the free energy differences associated with deprotonation reaction and free radical formation.

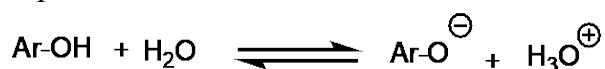
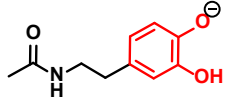
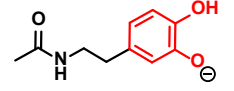
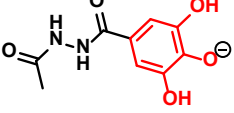
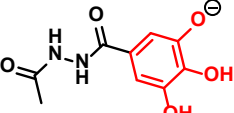


Table S1: Change in free energy (ΔG , kcal/mol) for the deprotonation reaction in DA and GA.

Molecular species	ΔG , kcal/mol	Computed pKa
	59.27	10.31
	52.53	9.14
	47.76	8.31
	49.79	8.66

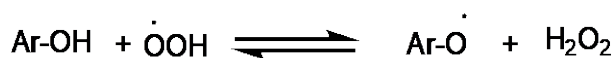


Table S2: Change in free energies for the radical formation

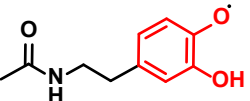
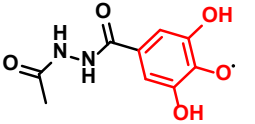
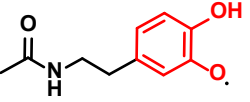
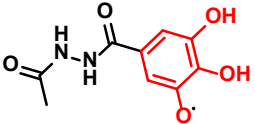
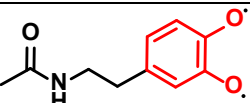
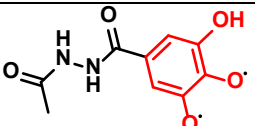
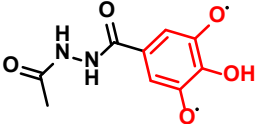
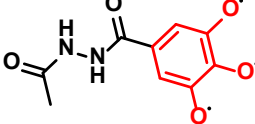
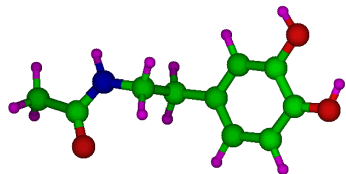
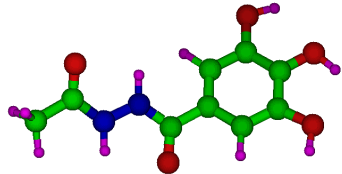
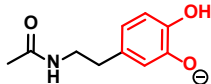
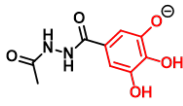
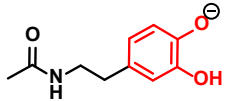
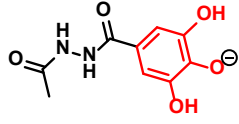
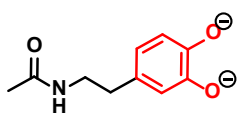
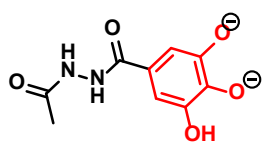
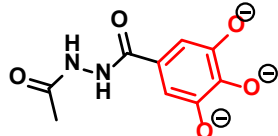
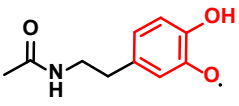
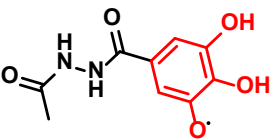
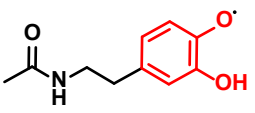
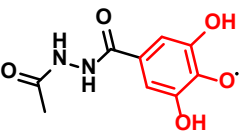
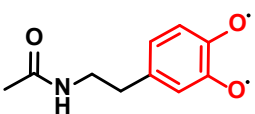
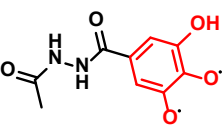
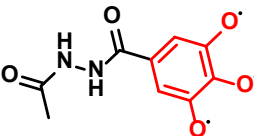
Molecular species	ΔG , kcal/mol	Molecular species	ΔG , kcal/mol
	-7.29		-6.61
	-6.10		-2.04
	+5.86		-0.778
			-3.78
			+16.53

Table S3: Energetics of charge, neutral and radical forms of GA and DA along with water, hydrogen peroxide, peroxide-free radical, and the hydronium ion. (Energy units in Hartrees)

	Energies without ZPE correction	Energies with ZPE correction	Energies without ZPE correction	Energies with ZPE correction
				
	DA-derivative		GA-derivative	
Ar(OH)-OH	-669.553664	-669.378074	-834.8774739	-834.729725
				
	Deprotonation-meta position		Deprotonation-meta position	
Ar(OH)-O ⁻	-669.0823232	-668.918664	-834.4098664	-834.274681
				
	Deprotonation-para position		Deprotonation-para position	
Ar(O ⁻)-OH	-669.0713013	-668.907919	-834.4134511	-834.277917
				
	Energetics of dianion		Energetics of dianion	
Ar(O ⁻)-(O ⁻)	-668.57294 (m,p)	-668.422324 (m,p)	-833.911688 (m,p) 833.9216299 (m,m)	-833.789381 (m,p) -833.798961 (m,m)
				
			Energetics of trianion	
Ar(O ⁻)(O ⁻)-(O ⁻)			-833.4058095 (m,m,p)	-833.295707 (m,m,p)

	 Energetics of free radical (meta-position)		 Energetics of free radical (meta-position)	
Ar(OH)-O \cdot	-668.923133	-668.759758	-834.2453534	-834.109322
	 Energetics of free radical (para-position)		 Energetics of free radical (para-position)	
ArO \cdot (OH)	-668.9176805	-668.754150	-834.2453534	-834.109322
	 Energetics of diradical		 Energetics of diradical	
Ar(O \cdot)-O \cdot	-668.2573784 (m,p)	-668.108237 (m,p)	-833.587253 (m,p) -833.5994131 (m,m)	-833.464845 (m,p) -833.477445 (m,m)
			 Energetics of triradical	
Ar(O \cdot)(O \cdot)- (O \cdot)			- 832.9301243(m,m,p)	- 832.822644(m,m,p)
	Energies of water, hydrogen peroxide, hydronium ion, and peroxide-free radical			
H ₂ O	-76.466463	-76.463565		
H ₃ O ⁺	-76.8550564	-76.839252		
HOO \cdot	-150.96473	-150.972778		
H ₂ O ₂	-151.6102822	-151.605591		

1.2 Synthesis of hydrazide derivative of gallic acid (GA-Hyd)

The hydrazide derivative of gallic acid was synthesized by esterification of the GA carboxylate followed by nucleophilic displacement with hydrazine according to the following procedure. Briefly, 4 g of GA was dissolved in 100 ml of methanol in a 250 ml round-bottom flask. To this solution, 12

drops of 98% sulfuric acid were carefully added and the reaction mixture was refluxed overnight under constant stirring. The mixture was cooled to room temperature, neutralized with saturated NaHCO₃ solution, and methanol was removed completely with reduced pressure using a rotary evaporator. The methyl gallate was extracted with ethyl acetate and the organic layer was collected and dried over anhydrous Na₂SO₄. The solution was evaporated and methyl gallate was obtained as a viscous liquid. To this flask, 60 ml of methanol and 2 drops of TEA were added and stirred for 30 min. Then 2 ml of 80% hydrazine monohydrate was added and the reaction mixture was stirred 48 h, at room temperature. The gallate hydrazide was obtained as a white suspension, which was filtered and washed 3 times with methanol and one time with water. The GA-hydrazide was obtained as an off-white solid with a 70% yield, which was dried overnight under a vacuum. The dried sample was pure as characterized by ¹H and ¹³C NMR spectroscopy.

Chemical shifts were measured in δ (ppm) with reference to the DMSO-d₆ solvent (δ = 2.50 ppm and 39.4 ppm for ¹H and ¹³C NMR, respectively). ¹H (500 MHz, DMSO-d₆, Figure S2), δ (ppm): 6.78 (s, 2H), 9.33 (s, 1H), 4.31 (s, 2H). The water peak in DMSO-d₆ appear at 3.73 ppm in place of 3.3 ppm is due to complexation with hydrazide group (this was separately verified by adding D₂O to this same NMR sample, data not shown). The phenolic peaks did not appear due to fast exchange of acidic protons with trace amounts of water in DMSO-d₆. ¹³C NMR (126 MHz, DMSO-d₆, Figure S3), δ (ppm): 166.3 (a), 123.3 (b), 106.3 (c), 145.4 (d), and 136.3 (e).

The attenuated total reflectance (ATR) FTIR spectra of GA-Hyd was further recorded on a Thermo Fisher Scientific Nicolet 6700 FTIR in the infrared region (4000–650 cm⁻¹) with 32 scans at a resolution of 4 cm⁻¹. The characteristic phenolic -OH stretching vibrations of gallol are present at 3297 cm⁻¹ to 3424 cm⁻¹.⁴ C=C stretching and bending vibrations bands for aromatic rings are present at 1543 cm⁻¹ and 1414 cm⁻¹ respectively.⁵ The bending vibrations of C-H in the ring and O-H of the phenol alcohol are mainly characterized by bands in the 1340-1050 cm⁻¹.^{4,5} The C=O stretching vibrations peak at 1602 cm⁻¹ and N-H bending vibrations peak at 1500 cm⁻¹ further confirms the formation of hydrazide derivative of gallic acid.

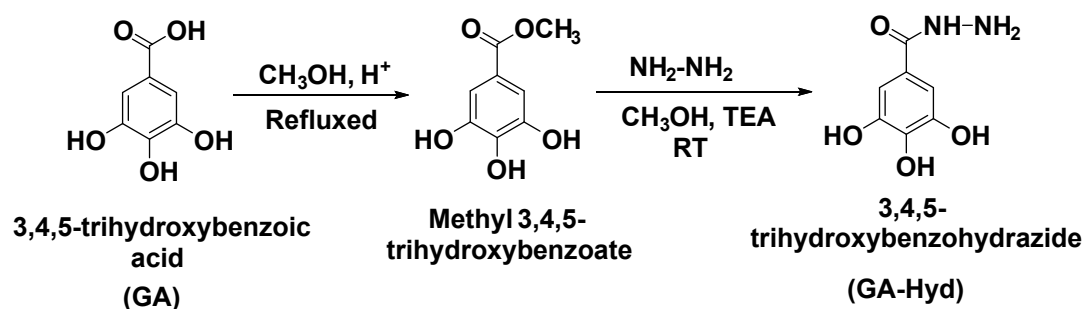


Figure S1: Synthesis of hydrazide derivative of gallic acid (GA-Hyd)

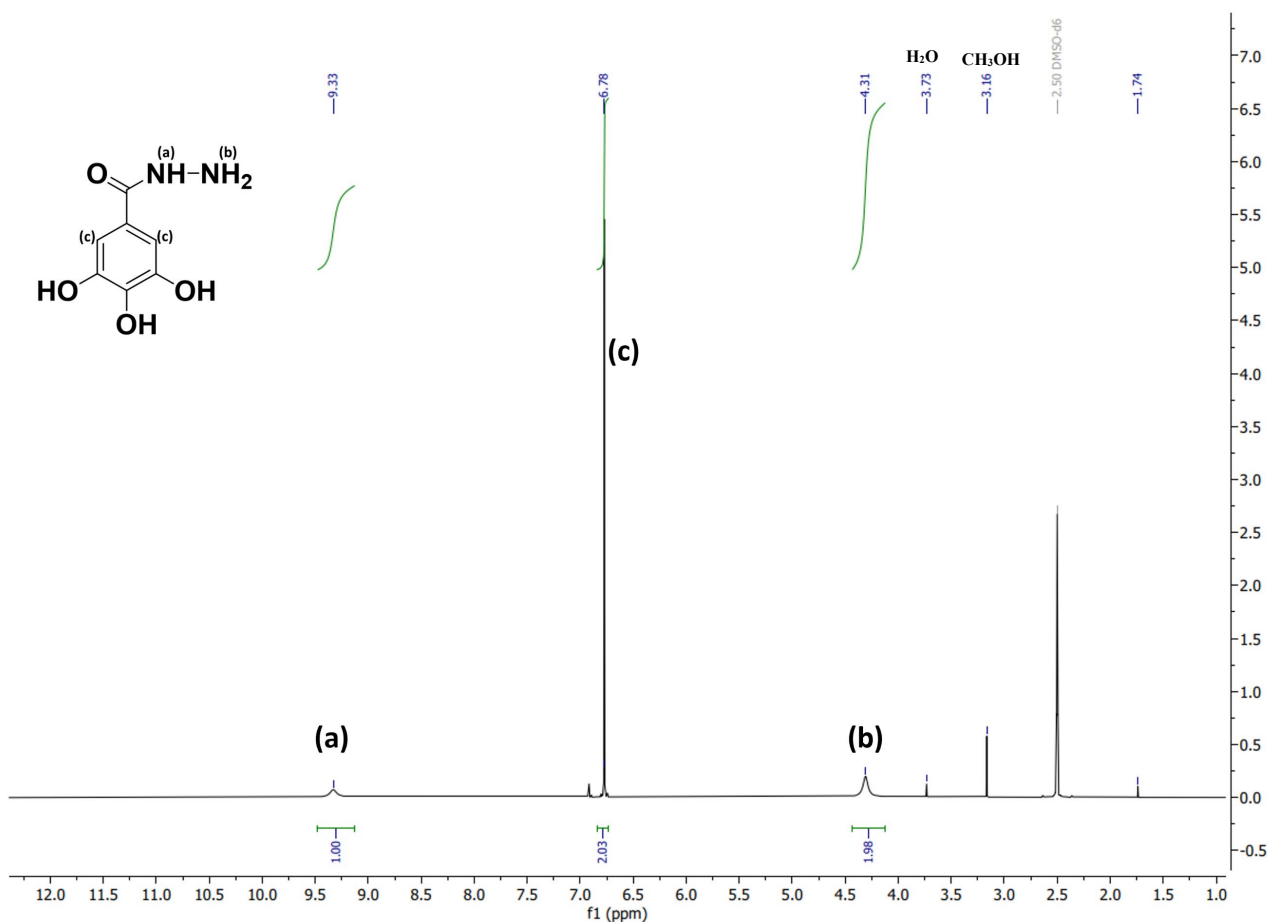


Figure S2: ¹H-NMR (500 MHz) spectra of hydrazide derivative of gallic acid (GA-Hyd) recorded in DMSO-d₆ at 298K.

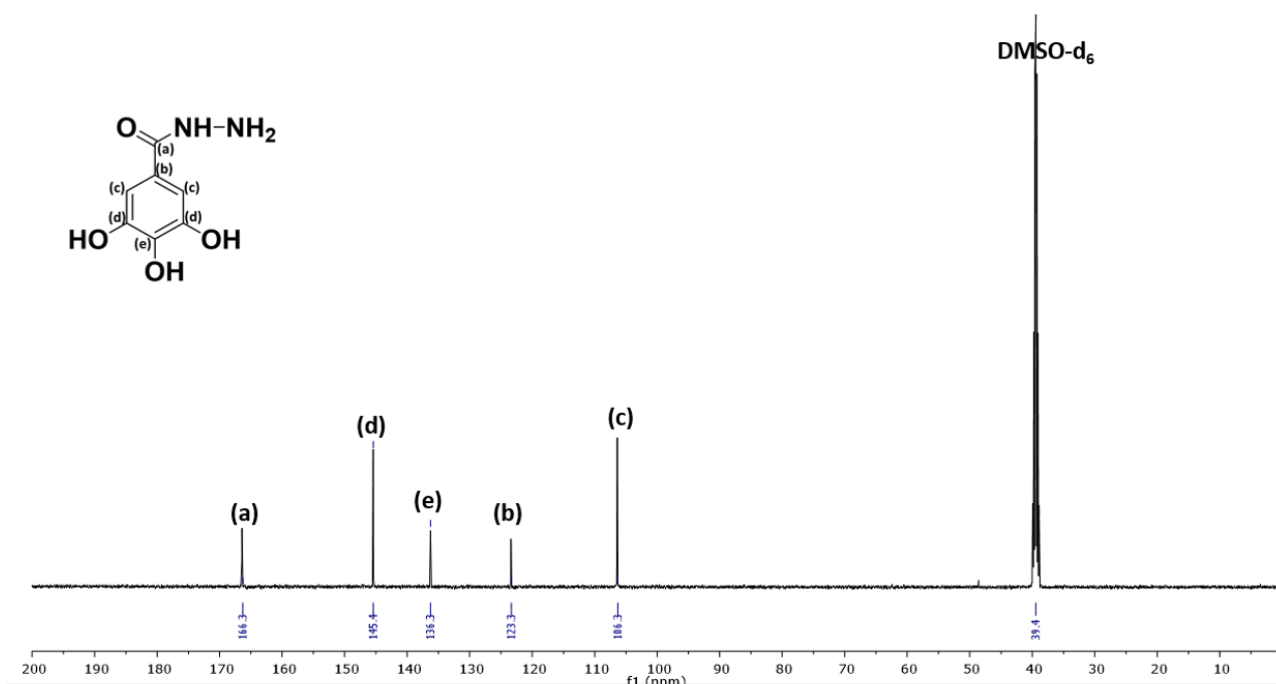


Figure S3: ¹³C-NMR (126 MHz) spectra of hydrazide derivative of gallic acid (GA-Hyd) recorded in DMSO-d₆ at 298K.

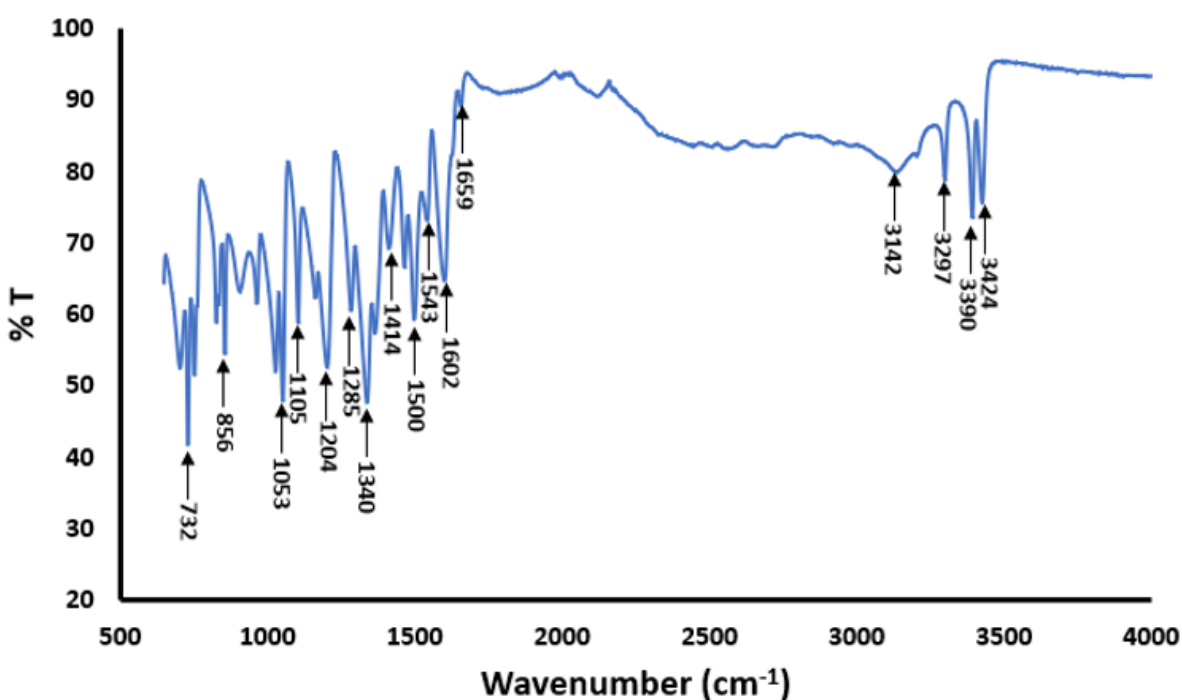


Figure S4: ATR-FTIR spectra of hydrazide derivative of gallic acid (GA-Hyd).

1.3 Synthesis of HA-GA conjugate

1 mmol of HA (400 mg, 1 equivalent) was dissolved in 75 mL of de-ionized water, to which 1 mmol of 1-hydroxy benzotriazole (HOBt, 153 mg, 1 equivalent) was added. This reaction mixture was stirred for 30 min. at room temperature. In another flask, 1 mmol hydrazide modified GA (GA-Hyd, 184 mg, 1 equivalent) was dissolved in 25 ml DMSO, which was subsequently added dropwise to the HA solution and was stir for another 30 min. The pH of the reaction solution was carefully adjusted to 4.8 with 1 M HCl and 1 M NaOH. Thereafter, 0.20 mmol EDC (19.20 mg, 0.10 equivalent) was added in one portion and was stirred overnight. The reaction mixture was then loaded into a dialysis bag (Spectra Por-6, MWCO 3500 g/mol) and dialyzed against dilute HCl (pH = 3.5) containing 100 mM NaCl (6 × 2L, 48 h) and then dialyzed against deionized water (4 × 2L, 24 h). Finally, the solution was lyophilized to obtain 375 mg white solid fluffy material in 94 % yield. The percentage of GA modification relative to the HA repeat units was estimated to be 4.5% as determined by integrating the aromatic peak at 6.89 ppm (green) of GA against the methyl peak of the N-acetyl of HA at 1.95 ppm (red).

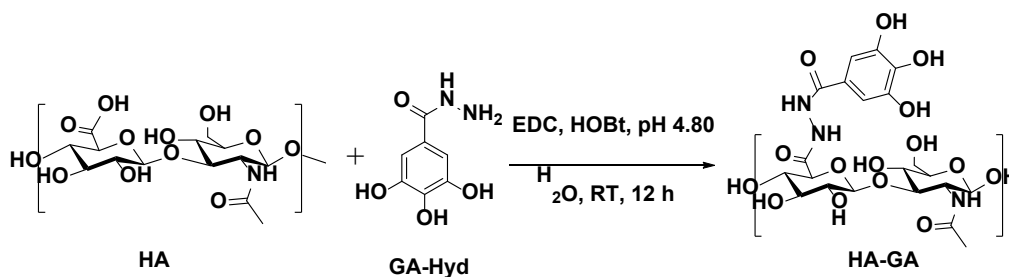


Figure S5: Synthesis of gallic conjugated hyaluronic acid (HA-GA)

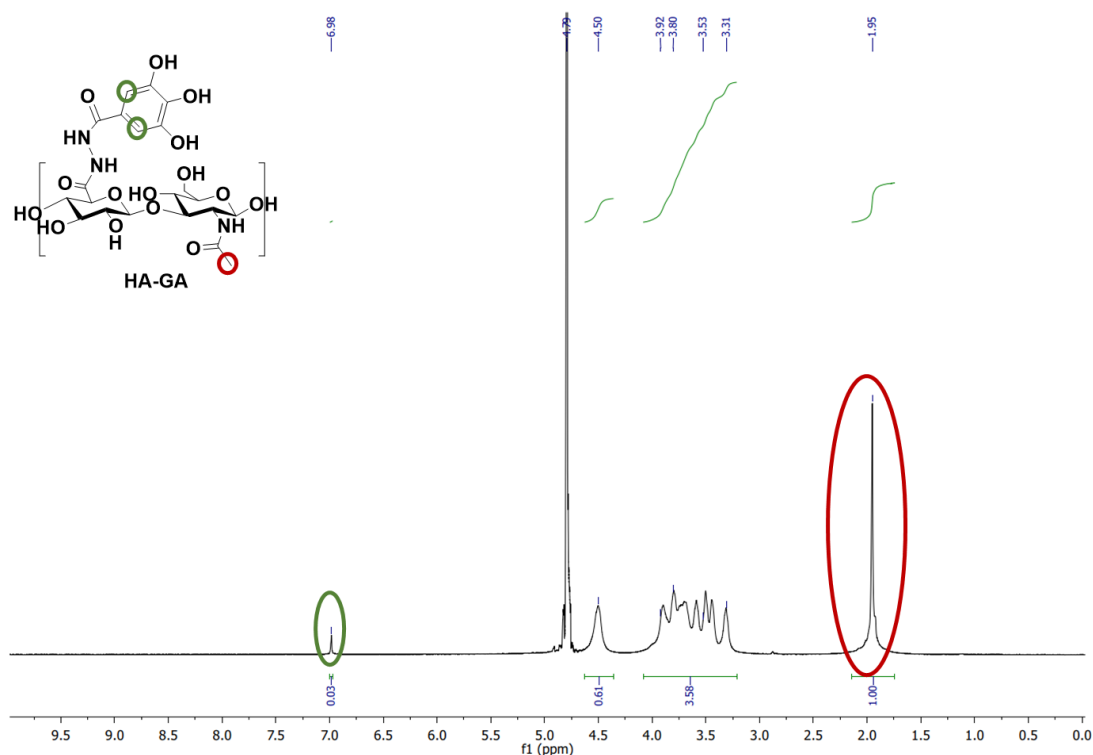


Figure S6: ^1H NMR spectrum of HA-GA recorded in D_2O at 298K.

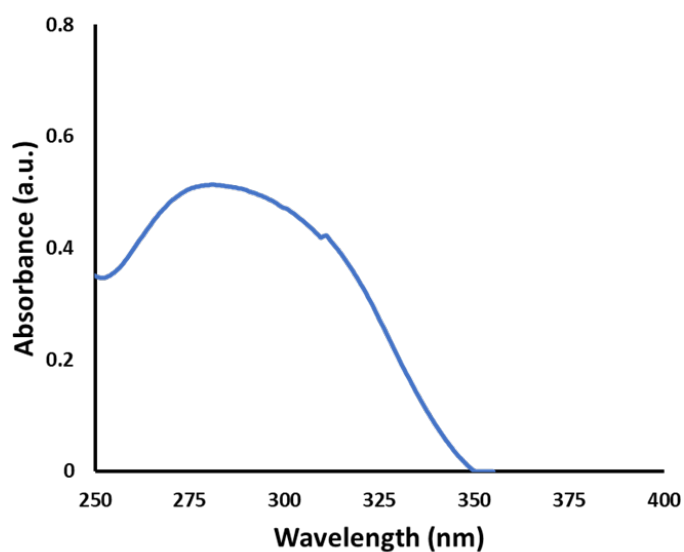


Figure S7: UV-Vis spectra of conjugated gallic modified hyaluronic acid (HA-GA)

The degree of modification was further ascertained by UV-Vis spectroscopy by dissolving HA-GA in 1x PBS at a concentration of 0.75 mg ml^{-1} and measuring the absorbance within 250-400 nm. The standard curve was established by dissolving GA into DMSO at a concentration of 5.8 mM and subsequently diluting in 1x PBS in the concentration range of 10-150 μM with a final DMSO concentration of $\sim 1\%$ in PBS. The degree of modification was ascertained to be 4.3 mol% with respect to the repeated disaccharide units of HA.

1.4 Synthesis of HA-DA conjugate

1 mmol of HA (400 mg, 1 equivalent), 1 mmol N-hydroxysuccinimide (NHS, 116 mg, 1 equivalent) and 0.25 mmol EDC (48 mg, 0.25 equivalent) was dissolved in degassed 75 mL de-ionized water. The pH of the reaction mixture was carefully adjusted to 5.5 with 1 M HCl and 1 M NaOH. Thereafter, 1 mmol of dopamine hydrochloride (95 mg, 0.5 equivalent) was added to the HA solution and the pH of the solution was maintained at 5.5 for 4 h and allowed to stir overnight. The reaction mixture was then loaded into a dialysis bag (Spectra Por-6, MWCO 3500 g/mol) and dialyzed against dilute HCl (pH = 3.5) containing 100 mM NaCl (6 × 2L, 48 h) and then dialyzed against deionized water (4 × 2L, 24 h). The solution was lyophilized to obtain white solid fluffy material.

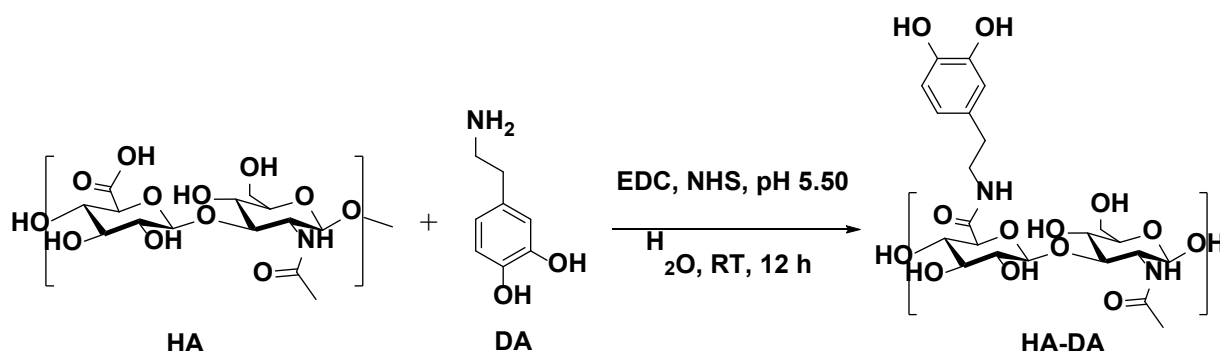


Figure S8: Synthesis of dopamine conjugated hyaluronic acid (HA-DA)

The degree of modification was ascertained by UV-Vis spectroscopy by dissolving HA-DA in 1x PBS at a concentration of 1.75 mg ml⁻¹ and measuring the absorbance within 250-350 nm. The standard curve was established over the concentration range of 50-400 μM by dissolving commercial dopamine hydrochloride into 1x PBS. The degree of modification was ascertained to be 4.6 mol% with respect to the repeated disaccharide units of HA.

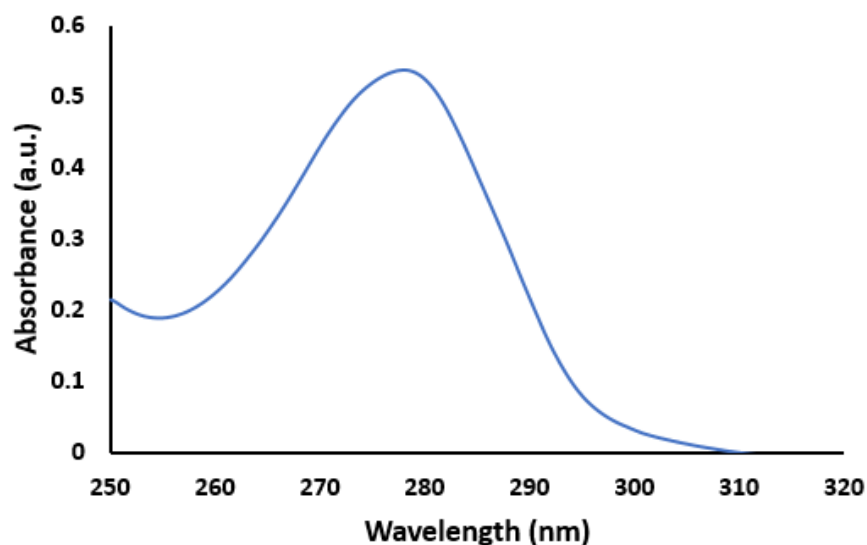


Figure S9: UV-Vis spectra of conjugated dopamine modified hyaluronic acid (HA-DA)

The conjugation of DA on the HA backbone was further confirmed by NMR spectroscopy. The percentage of DA modification relative to the HA repeat units was estimated to be ~5% (similar to UV-based estimation) as determined by integrating the aromatic peaks at 6.82, 7.18, and 7.38 ppm (blue) of DA against the methyl peak of the N-acetyl of HA at 1.96 ppm (red).

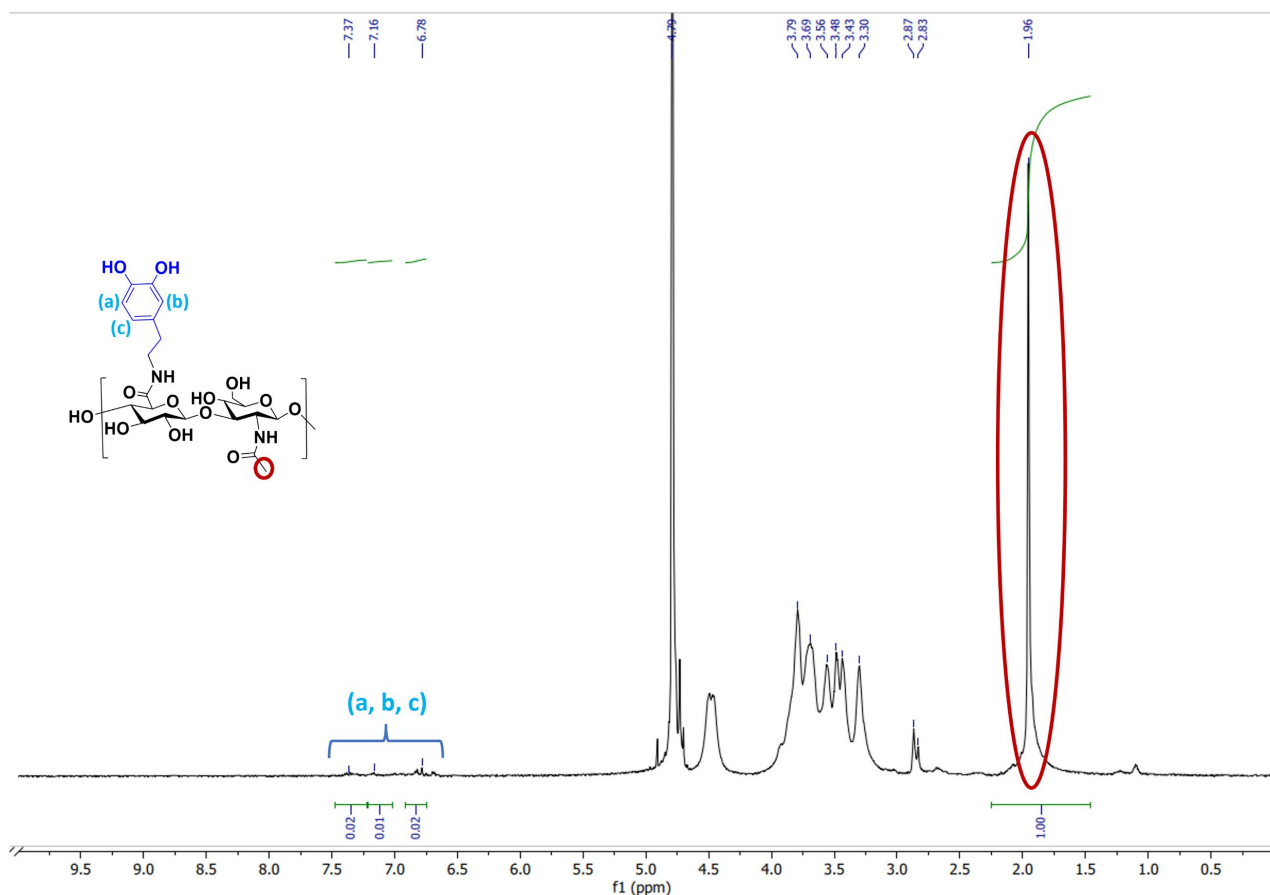


Figure S10: ^1H NMR spectrum of HA-DA recorded in D_2O at 298K.

We have further supported the conjugation of DA and GA on hyaluronic acid by FTIR spectroscopy. Attenuated total reflectance (ATR) FTIR spectra were recorded on a Thermo Fisher Scientific Nicolet 6700 FTIR in the infrared region ($4000\text{--}650\text{ cm}^{-1}$) with 32 scans at a resolution of 4 cm^{-1} .

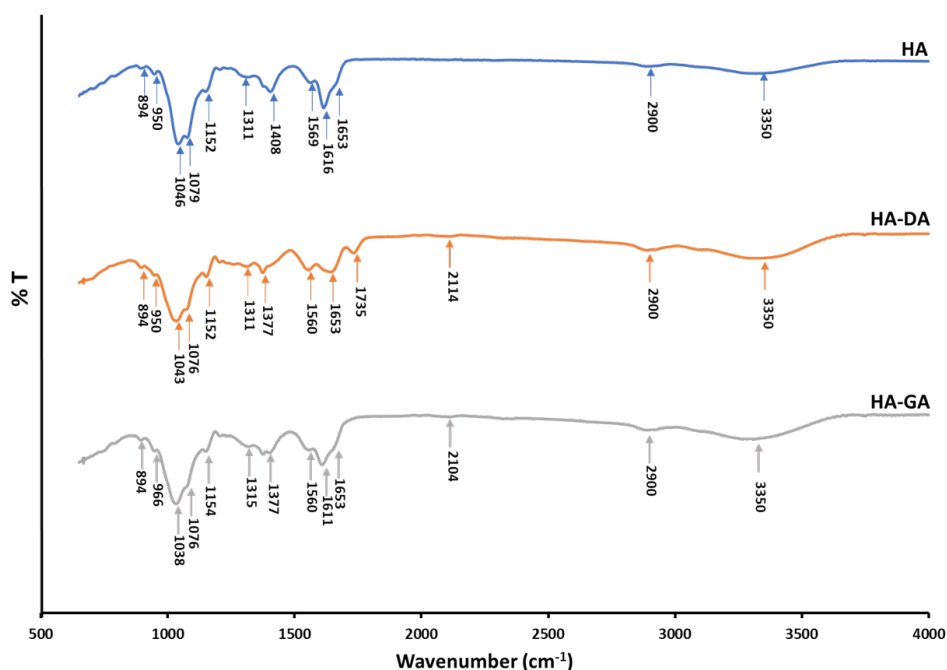


Figure S11: ATR-FTIR spectra of hyaluronic acid (HA), conjugated dopamine modified hyaluronic acid (HA-DA), and conjugated gallic modified hyaluronic acid (HA-GA)

All the HA, HA-DA, and HA-GA show a broad peak at 3100-3600 cm^{-1} due to the intramolecular and intermolecular stretching vibrations of hydroxyl groups. The peaks around 1035-1151 cm^{-1} ascertain the C-O-C hemiacetal saccharide units in the backbone. The symmetrical vibrational stretching of $-\text{CH}_2$ group at 2900 cm^{-1} , asymmetric stretching of $-\text{COO}^-$ the carboxylic acid around 1377-1408 cm^{-1} , and the bands around 1560-1611 cm^{-1} due to the amide I and II are also present in all three polymers. In the case of HA-DA, the characteristic $-\text{C}=\text{O}$ stretching of amide bond due to conjugation of dopamine on carboxyl group of HA appears at 1735 cm^{-1} .^{6,7}

1.5 Estimation of the ratio of anionic and neutral DA and GA at neutral pH

Using the pK_a estimated by spectrophotometric method, the ratio of neutral or anionic species was estimated at pH 7.4 following the Henderson-Hasselbalch equation. For example, to estimate the ratio of [DA] to $[\text{DA}^-]$, the following equation was used

$$\text{pH} = \text{pK}_a - \log\left(\frac{[\text{DA}]}{[\text{DA}^-]}\right)$$

$$\log\left(\frac{[\text{DA}]}{[\text{DA}^-]}\right) = \text{pK}_a - \text{pH}$$

$$\log\left(\frac{[\text{DA}]}{[\text{DA}^-]}\right) = 7.42 - 7.4$$

$$\log\left(\frac{[\text{DA}]}{[\text{DA}^-]}\right) = 0.02$$

$$\left(\frac{[\text{DA}]}{[\text{DA}^-]}\right) = 1.047 \text{ or } 52:48 \text{ ratio}$$

1.6 pKa determination

We followed a reported spectrophotometric protocol to determine the pKa of HA-DA and HA-GA conjugates.⁸ Briefly, HA-DA and HA-GA conjugates were dissolved in 1 mM aqueous HCl solution containing 0.1 M NaCl at a concentration of 0.5 mg/ml. Thereafter, 0.01M NaOH solution was added incrementally and stirred for 10 min. and the pH was recorded. The absorbance of the pH stabilized HA-DA and HA-GA solutions were sequentially recorded at 295 nm and 325 nm respectively. With the increase in pH, the absorbance increased, indicating the formation of quinone intermediate. The pKa value was obtained by plotting the $-\log[(A_{\max} - A_i)/A_i]$ as a function of the pH. The pKa values are displayed where the linear fit crosses the abscissa

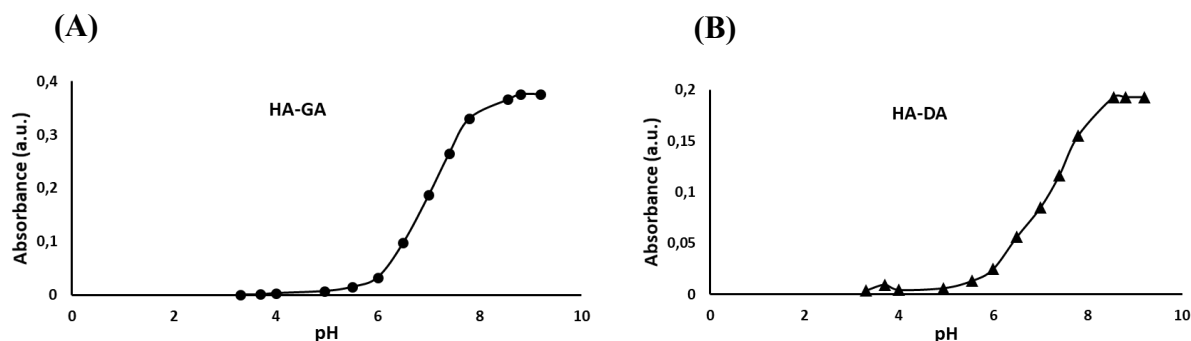


Figure S12: Absorbance of (A) HA-GA and (B) HA-DA as a function of Ph

1.7 Antioxidant property

The antioxidant property of DA, GA HA-DA, and HA-GA conjugates were quantified using DPPH (2,2,1-diphenyl-1-picrylhydrazyl) radical scavenging assay.⁹ Briefly, 12.5 μ M solution of DA or GA in water or 25 μ M of HA-DA or HA-GA conjugates (calculated relative to the % of DA or GA grafted on the HA polymer) were prepared by dissolving an appropriate amount of test materials in deionized water. To this aqueous solution, an equal volume of a DPPH in methanol solution (1 mg/12.5 ml) was added and the mixture was incubated for 30 min. at room temperature, and the absorbance of the resulting solution was measured at 517 nm using a UV-Vis spectrophotometer.

The DPPH scavenging activity (%) = $\left[\frac{(A_0 - A_1)}{A_1} \right] \times 100$,

Where, A_0 is the absorbance of a blank DPPH solution that was used under the same reaction conditions in the absence of synthesized polymers or small molecules, and A_1 is the absorbance of DPPH solution in the presence of polymer samples or small molecules. All the experiments were done in triplicates in two independent experiments.

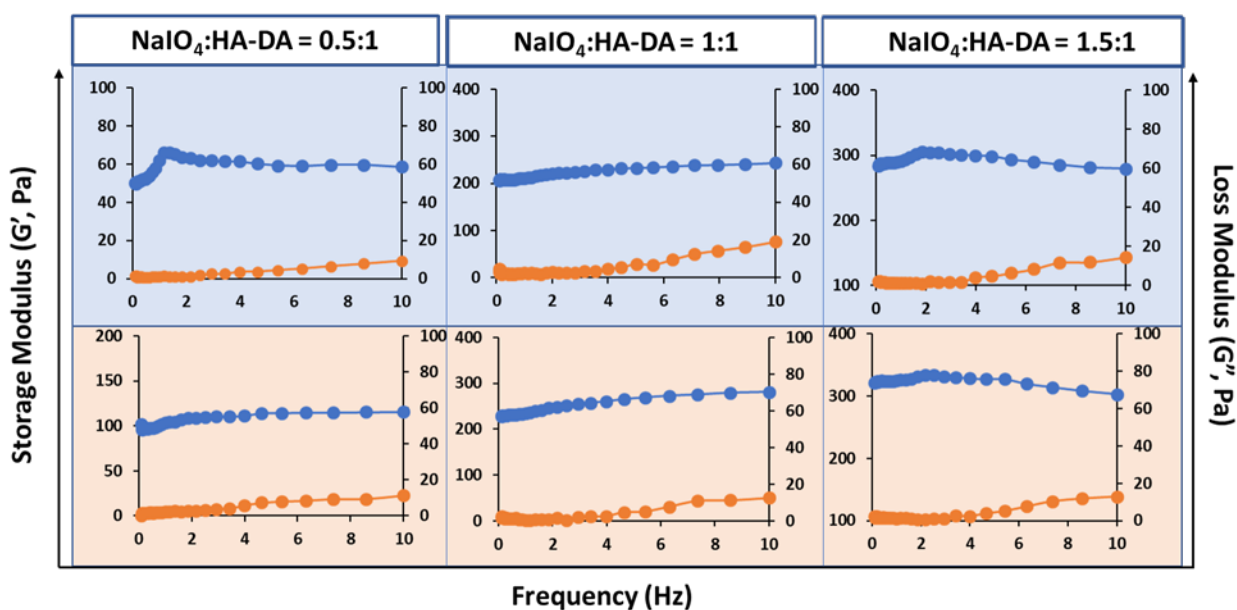
1.8 Hydrogel preparation

The HA-DA hydrogels were prepared by crosslinking dopamine moieties of the hyaluronic acid. First, HA-DA was dissolved in 1x PBS at 1.6 weight% (16 mg/ml). For basic condition mediated gels, the pH of the solution was adjusted to 8.6 by 0.1 M NaOH solution and for neutral gels, the pH of the dissolved solution was adjusted to 7.4. Further, 25 μ l of NaIO₄ at four different concentrations (at a ratio of 0.1, 0.5, 1, and 1.5 moles to 1 mole of HA-DA) in 1x PBS was homogeneously mixed to HA-DA solution (4 mg/225 μ l) to form the gels. The same protocol was followed for HA-GA gels under neutral conditions. For basic pH conditions, the NaIO₄ was dissolved in 1x PBS pH 9.0 to obtain the final gel pH 8.4. Without the addition of periodate, HA-DA didn't form gels at basic

condition, however, we obtained soft gels when we adjusted the dissolved HA-GA solution pH to 8.4. This gelation couldn't be observed when we used degassed 1x PBS. Before hydrogel formation, the materials were UV sterilized for 20 minutes and subsequently dissolved in sterile solutions.

1.9 Rheological properties

To study the oscillatory rheological property, hydrogels (1.6wt%, 250 μ l) were prepared in the form of cylinders with a 12 mm diameter. The gels were cured overnight, and the rheological property was measured using a TA instruments' TRIOS Discovery HR 2 rheometer. Amplitude sweep, also defined as dynamic stress sweep, was first performed to determine the linear viscoelastic region (LVR) over a stress or strain range keeping the frequency constant, indicating the stability of the overall material. The wider the LVR, the more stable and viscoelastic are the materials. While the applied force becomes too high, the structural integrity collapse and storage modulus (G') value decrease, and loss modulus (G'') value increase indicating more flow or liquid-like behavior of the materials. The amplitude sweep consisted of the varying amplitude of deforming force while maintaining a constant frequency value of 1 Hz and was used to determine the strain value for the subsequent frequency sweep. The frequency sweep consisted of varying frequency of the deforming force, between 0.1 and 10 Hz with a constant strain value of 1% as determined from the amplitude sweep. The values for storage (G') and loss (G'') modulus, which quasi-defines the elastic or solid-like behavior and flow or liquid-like behavior respectively within the viscoelastic materials, were obtained using the frequency sweep and were plotted against the frequency (Hz).



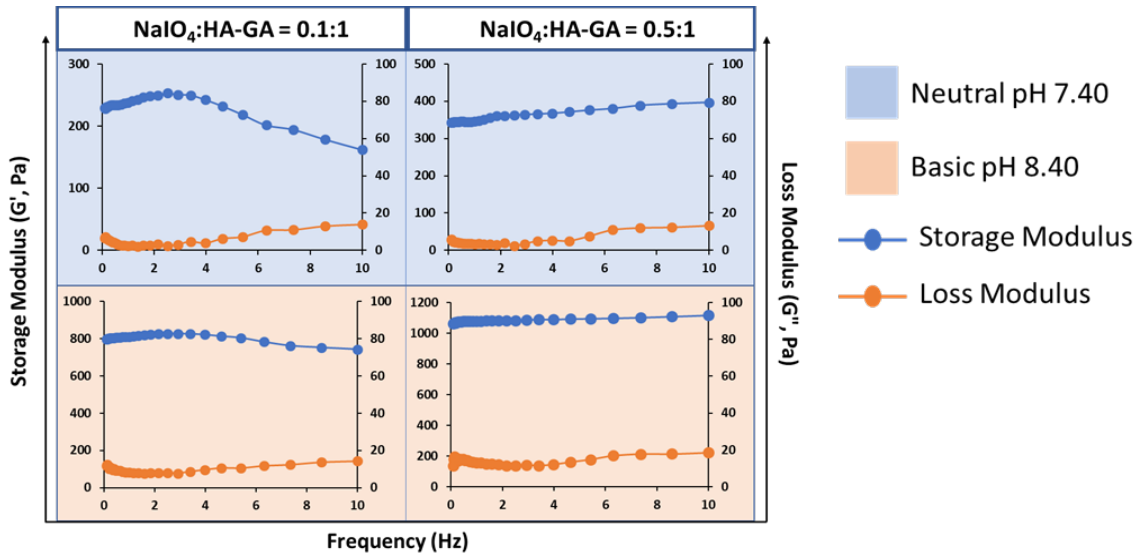


Figure S13: Rheological characterizations of HA-DA and HA-GA hydrogels synthesized at neutral pH 7.4 and basic pH 8.4 at different periodate concentrations

1.10 Enzymatic stability Study

To substantiate the effect of crosslinking on enzymatic degradation and swelling of the hydrogels, a study was performed using hyaluronidase at a concentration of 25 U/mL in PBS at pH 7.4. Five parallel samples of 250 μ L HA-DA and HA-GA gels were prepared in glass vials of known blank weight, allowed to crosslink for 24 hours, weighed with the formed gels, and subsequently submerged in 1 mL hyaluronidase PBS solution. To compare the results, we chose gels with similar storage modulus (\sim 340 Pa; 1.5:1 NaIO₄:HA-DA and 0.1:1 NaIO₄:HA-GA, pH 8.4), and the third group was HA-GA gel with higher storage modulus (\sim 800 Pa; 0.5:1 NaIO₄:HA-GA, pH 7.4). The hyaluronidase buffer solution was carefully removed prior to measurement every time point, the gels were weighed, and the enzyme buffer was replaced after each measurement. The degradation weight percentage was calculated using the formula:

$$\text{Remaining weight \%} = \left(\frac{\text{Measured Weight}}{\text{Initial Weight}} \right) \times 100$$

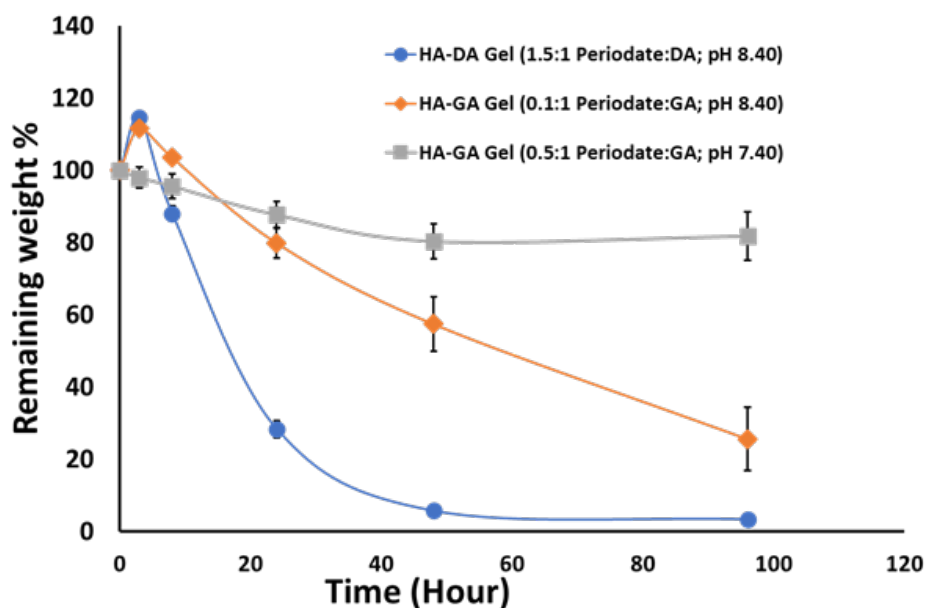


Figure S14: Enzymatic degradation and swelling study of HA-DA and HA-GA hydrogels at different periodate concentrations in presence of 25 U/mL hyaluronidases.

1.11 Tissue-adhesive Tack Test

To observe the difference in the tissue adhesive property of the two hydrogels (HA-DA and HA-GA), a tack adhesion test was performed using the rheometer. We used porcine muscle tissue that was obtained from a local abattoir. The muscle tissue was sectioned into 12 mm discs before use. We first glued the porcine muscle having the same diameter as that of the geometry (12 mm) to the movable top head of the rheometer and then placed the fully cured 250 μ l of HA-HA and HA-GA gels of 2 mm thickness on the bottom plate. Subsequently, the top plate attached with the muscle tissue was placed in contact with the gel with a holding period of 120 seconds (residence time) where a constant compressive force of 50 mN was applied in order to establish a uniform molecular contact between the tissue and the gels. Thereafter, the top plate was pulled up at a constant velocity of 10 μ m/sec to record the change in axial force (N) with respect to time. The experiments were performed in triplicates at 25 °C. A graph of axial force (N) vs step time was plotted to observe differences between the two hydrogels.

1.12 Cell culture

Human fibroblast cells (CRL-2429) cells were cultured in Dulbecco's Modified Eagle Medium (DMEM, Gibco) with 10% fetal bovine serum and 1% Penicillin-Streptomycin (Gibco) at 37 °C and 5% CO₂. THP-1 cells (human monocytic cell line) were cultured in Roswell Park Memorial Institute (RPMI) 1640 medium (Gibco) with 10% fetal bovine serum (FBS) and 1% Penicillin-Streptomycin at 37 °C and 5% CO₂.

1.13 Live/Dead staining

For live/dead staining, CRL-2429 cells were encapsulated in 250 μ l of HA-DA and HA-GA hydrogels that were formulated with 1.5:1 NaIO₄: DA ratio at pH 8.4 and 0.1:1 NaIO₄: GA ratio at pH 7.4 respectively to obtain gels of comparable viscoelastic properties. The CRL-2429 cells were cultured at a concentration of 2x10⁶ cells/ml in a 48-well plate. The encapsulated cells were cultured for 7

days, with a medium change every alternate day, and cell viability, as well as changes in the morphology of the cells, was visualized by LIVE/DEAD staining (Viability/Cytotoxicity Kit for mammalian cells, Molecular Probes, USA) using a fluorescence microscope. To carry out the Live/Dead staining, the medium was aspirated from the wells and the gels were washed with 1x PBS twice. 300 μ l Live/Dead staining solution containing 2 μ M Calcein AM and 1 μ M Ethidium homodimer in 1X PBS was added to the wells and the plates were incubated at 37°C for 1.5 hours. Post incubation, the hydrogels were washed with 1X PBS once and imaged using a 10x objective on Nikon Eclipse Ts 2 fluorescence microscope. Live/Dead staining was performed on days 1, 4, and 7 after the hydrogels were made. Images obtained from the microscope were post-processed using Nikon NIS Viewer and ImageJ software.

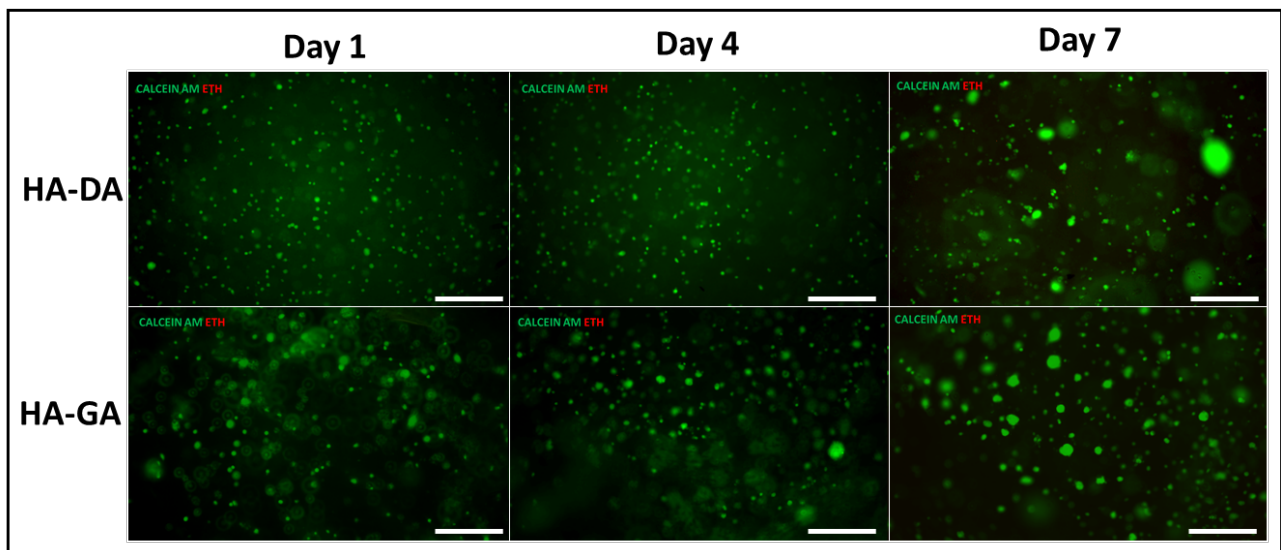


Figure S15: Live/Dead staining of CRL-2429 cells encapsulated inside hydrogels on 1,4 and 7 days of culture. Cells stained in green (Calcein AM) represent live cells while cells stained in red (ETH) represent dead cells. Both gels showed a high number of live cells for 7 days of culture.

1.14 Macrophage study

THP-1 cells, 80000 in number were added to 24 well plates. Free DA and free GA at the concentration of 120 μ g/ml were added to the cells. 4 mg/ml of HA-DA and HA-GA (both were added such that the amount of DA and GA was equivalent to 120 μ g/ml) was added to the cells. 4 mg/ml of HA was also added as a separate group. The cells were exposed for 8 days to the materials after RNA was isolated for the qRT-PCR. RNeasy Plus Mini Kit (Qiagen) was used for RNA extraction. Post extraction, the RNA samples were stored at -20 °C. The concentration and quality of RNA were measured using NanoDrop 2000 microvolume spectrophotometer (Thermo Fisher Scientific). cDNA was prepared by following the Maxima First Strand cDNA synthesis kit (K1671, Thermo Fisher Scientific). For qPCR reactions, TaqMan Fast Advanced Master Mix (Thermo Fisher Scientific), and TaqMan assay primers were subjected to the reaction process in a Bio-Rad CFX96 real-time PCR machine. The expression levels of the following genes were analyzed using commercially available TaqMan Gene Expression Assays (Thermo Fisher Scientific): TNF (Hs00174128), IL-8 (CXCL8) (Hs00174103), IL-1Ra (Hs00893626), IL-1 β (Hs01555410), with β -actin (ACTB) (Hs01060665) as the housekeeping gene.

References

1. Barone, V. & Cossi, M. Quantum calculation of molecular energies and energy gradients in solution by a conductor solvent model. *J. Phys. Chem. A* **102**, 1995–2001 (1998).
2. Schaftenaar, G. & Noordik, J. H. Molden: A pre- and post-processing program for molecular and electronic structures. *J. Comput. Aided Mol. Des.* **14**, 123–134 (2000).
3. Gaussian 09 Citation | Gaussian.com.
4. Shandil, A. *et al.* Targeting keratinocyte hyperproliferation, inflammation, oxidative species and microbial infection by biological macromolecule-based chitosan nanoparticle-mediated gallic acid–rutin combination for the treatment of psoriasis. *Polym. Bull.* **77**, 4713–4738 (2020).
5. Aydogdu, A., Sumnu, G. & Sahin, S. Fabrication of gallic acid loaded Hydroxypropyl methylcellulose nanofibers by electrospinning technique as active packaging material. *Carbohydr. Polym.* **208**, 241–250 (2019).
6. Hong, S. *et al.* Hyaluronic Acid Catechol: A Biopolymer Exhibiting a pH-Dependent Adhesive or Cohesive Property for Human Neural Stem Cell Engineering. *Adv. Funct. Mater.* **23**, 1774–1780 (2013).
7. Vasi, A. M., Popa, M. I., Butnaru, M., Dodi, G. & Verestiuc, L. Chemical functionalization of hyaluronic acid for drug delivery applications. *Mater. Sci. Eng. C* **38**, 177–185 (2014).
8. Bermejo-Velasco, D., Azémar, A., Oommen, O. P., Hilborn, J. & Varghese, O. P. Modulating Thiol p K_a Promotes Disulfide Formation at Physiological pH: An Elegant Strategy to Design Disulfide Cross-Linked Hyaluronic Acid Hydrogels. *Biomacromolecules* **20**, 1412–1420 (2019).
9. Lai, J. Y. & Luo, L. J. Antioxidant gallic acid-functionalized biodegradable in situ gelling copolymers for cytoprotective antiglaucoma drug delivery systems. *Biomacromolecules* **16**, 2950–2963 (2015).